Supplementary Information

Measurements for Molar Extinction Coefficients of Aqueous Quantum Dots

Chaoqing Dong, Jicun Ren*

College of Chemistry & Chemical Engineering, State Key Laboratory of Metal Matrix Composites, Shanghai Jiaotong University, 800 Dongchuan Road, Shanghai 200240, P. R. China

E-mail: jicunren@sjtu.edu.cn

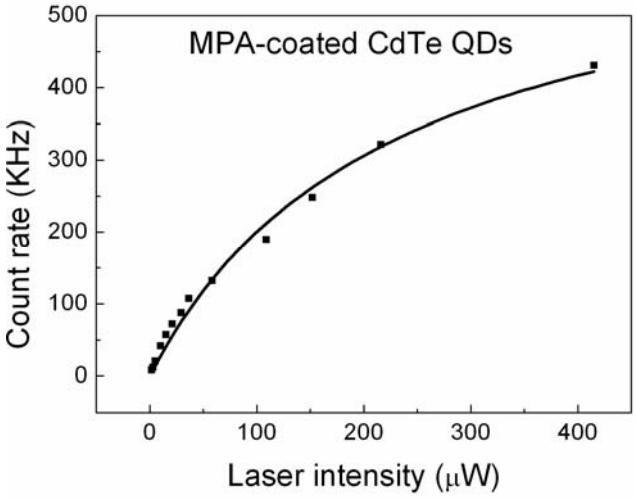

Fig. S1 Observed average count rate of QDs as a function of laser intensity. Saturation intensities (I_{sat}) are extracted by fitting the data to a saturation function $CR=CR_0*I/(I+I_{sat})$.

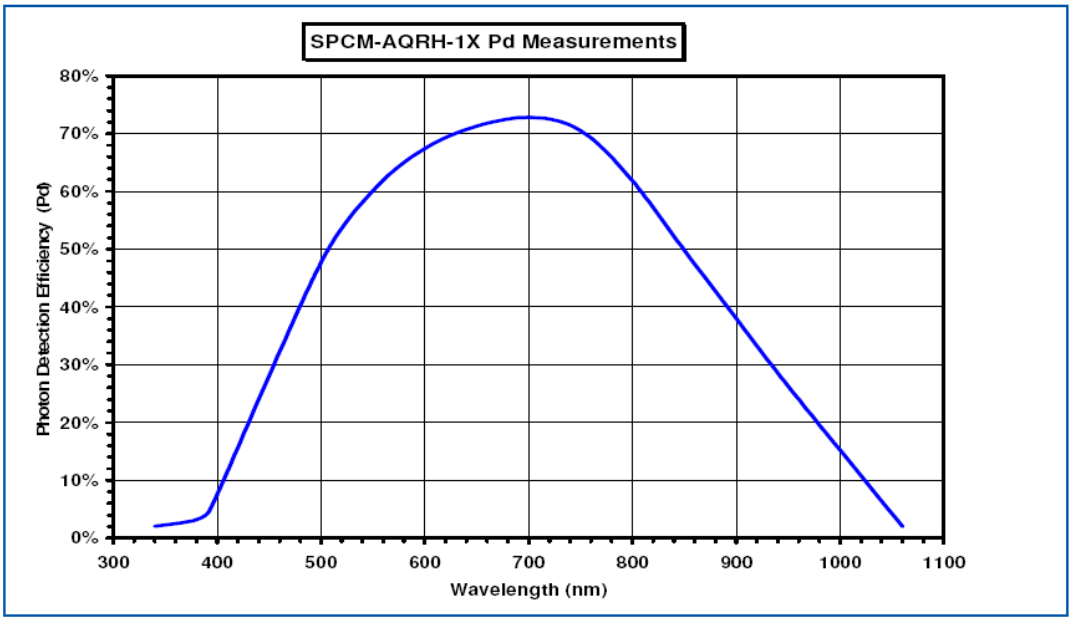

Fig. S2. Typical photon detection efficiency (Pd) vs. wavelength. The figure was subtracted from Perkin Elmer's website (www.optoelectronics.perkinelmer.com).

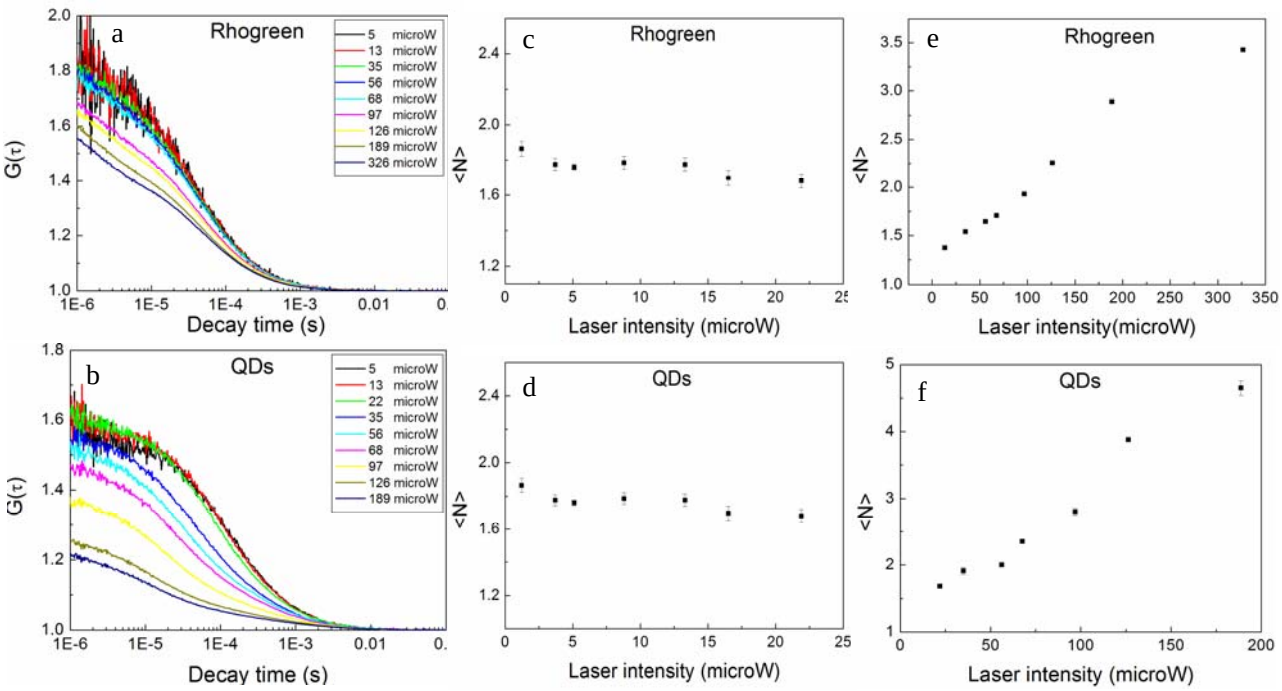

Fig. S3. (a) (b) Autocorrelation curves of Rhogreen and QDs at different laser intensity. Figure S3(c) (d) shows change of number of fluorescent Rhogreen molecules in detection volume with laser intensity. Fig.S3 (e) (f) shows change of number of bright QDs in detection volume with laser intensity.

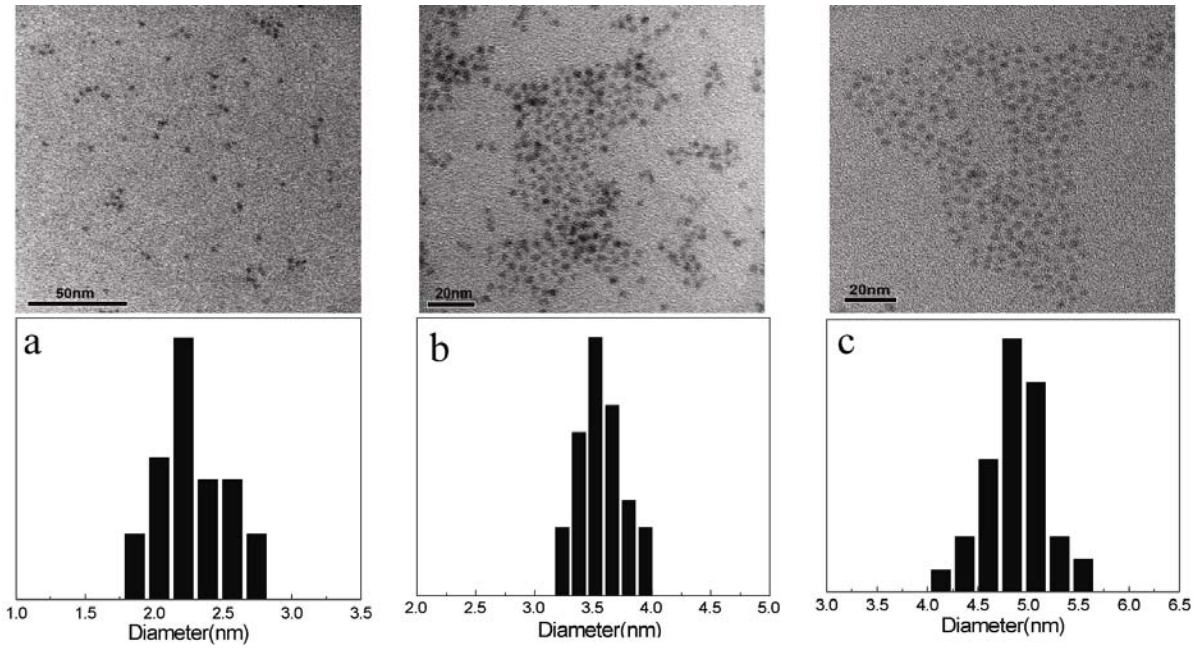

Fig. S4. (a)(b)(c) TEM pictures and diameter distribution histogram of QDs, whose emission peak position were at 532nm, 595nm and 604nm, respectively.

Effect of polydispersity of QDs on G (0)

Here the influence of brightness polydispersity on G (0) was studied by investigated the effect of size polydispersity of QDs on brightness of QDs using QD595 as an example. The TEM figure and size distribution of QD595 was show in the Fig. s4. The percentage of QDs, whose diameter was at 3.2 nm, was about 27% (here they were regarded as component 1). The percentage of QDs, whose diameter was at 3.5 nm, was about 53% (here they were regarded as component 2). The percentage of QDs, whose diameter was at 3.8 nm, was about 20% (here they were regarded as component 3). Deduced from eq. 9($BPP = k \times \varepsilon$) and eq.14 ($\varepsilon_{488\mathrm{nm}} = 1745 d^{2.66}$), the BPP of QDs is proportionally to $d^{2.66}$. So if we assumed BPP of QDs with diameter of 3.8 nm as 1.0, BPP of QDs with diameter of 3.2 nm and 3.5 nm are 0.63 and 0.80, respectively. As we know, when there are multiple diffusion components with different brightness, the FCS function should be described as following equation.

$$G(\tau) = \frac{1}{(\sum \mathrm{Q_k} N_k)^2} \cdot \sum \mathrm{Q_j^2} N_j \cdot \frac{1}{(1 + \frac{\tau}{\tau_{D,j}})} \cdot \frac{1}{\sqrt{1 + (\frac{\omega_0}{z_0})^2 \cdot \frac{\tau}{\tau_{D,j}}}}$$

Here Q_1, N_1 for component 1 are 0.63, 0.27. Q_2, N_2 for component 2 are 0.80, 0.53. Q_3, N_3 for component 3 are 1.00, 0.20. If we assumed that the QDs sample was composed of three components (component 1, 2, 3), the FCS curve of QDs simulated using above equation should be the red line in Fig. S5. If we assumed QDs sample as single component (component 2), which was adopted in our manuscript, the FCS curve of QDs should be the dark line in Fig. S5. The minor difference of G (0) showed that the effect of polydispersity of QDs on G (0) was negligible.

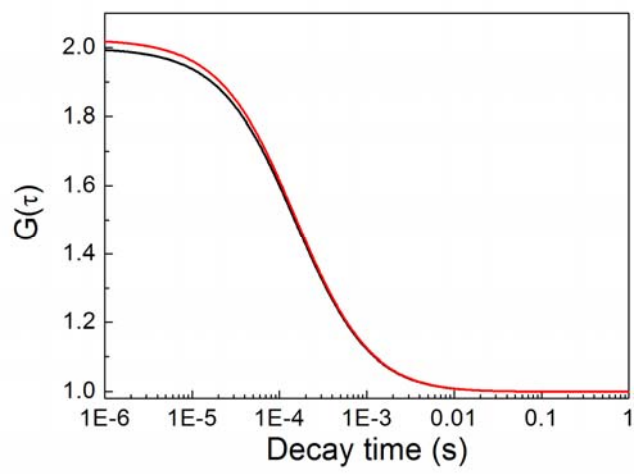

Fig. S5. Effect of polydispersity of QDs on G (0).

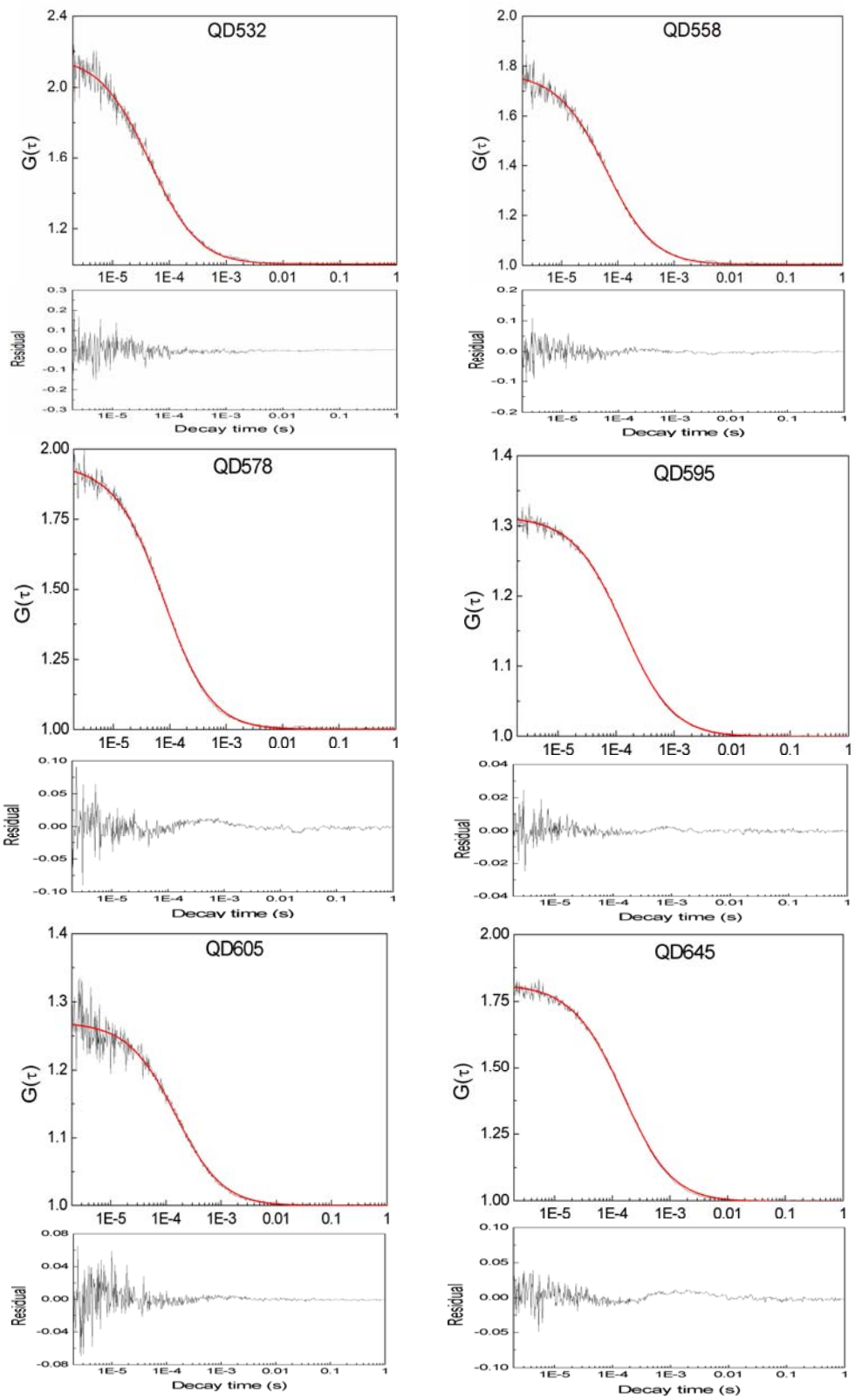

Fig. S6. The autocorrelation curves, fitting curves and residual curves of different QDs. The red curves were fitted using the following equation.

$$G(\tau) = \frac{1}{N} \cdot \frac{1}{(1+\frac{\tau}{\tau_D})} \cdot \frac{1}{\sqrt{1+(\frac{\omega_0}{z_0})^2 \cdot \frac{\tau}{\tau_D}}}$$

Table S1 PL emission peak positions and according PL QYs of QDs at different reaction time prepared from different monomer concentration solutions

monomer concentration (1 mM)			monomer concentration (3 mM)			monomer concentration (10 mM)		
Reaction time (hrs)	PL emission (nm)	PL QY	Reaction time (hrs)	PL emission (nm)	PL QY	Reaction time (hrs)	PL emission (nm)	PL QY
3	532	0.482±0.025	4	539	0.277±0.014	3	545	0.112±0.025
6	558	0.618±0.031	8.5	557	0.315±0.004	4	549	0.106±0.028
9	578	0.541±0.041	13.5	575	0.311±0.019	7	562	0.125±0.032
12	595	0.526±0.045	26.5	625	0.235±0.027	13	582	0.144±0.025
14	604	0.477±0.038	31.5	637	0.214±0.033	24	612	0.151±0.022
23	636	0.290±0.028	37.5	649	0.194±0.033	31	628	0.140±0.035
26	640	0.264±0.035				37	643	0.125±0.021
29	645	0.254±0.044						